ELSEVIER

Chemical Engineering Journal 140 (2008) 130–135

Chemical Engineering Journal

www.elsevier.com/locate/cej

Kinetic study on regeneration of $Fe^{II}EDTA$ in the wet process of NO removal

Zhong Biao Wu, Li Wang, Wei Rong Zhao *

Department of Environmental Engineering, Zhejiang University, Hangzhou 310027, China

Received 15 April 2007; received in revised form 6 September 2007; accepted 18 September 2007

Abstract

Cyclic voltammetry, quasi-steady-state polarization curves and potentiostatic step method were applied to study the regeneration of $Fe^{II}EDTA$ in the wet process of NO removal. The results showed that the $Fe^{III}EDTA$ reduction was a fast reversible process with one electron transferred on Pt electrode surface. Standard rate constant k^0 of $Fe^{III}EDTA$ reduction at 298 K was found to be 0.0263 cm s^{-1}. According to the calculated diffusion activation energy of 24.93 kJ mol^{-1}, apparent activation energy of 25.74 kJ mol^{-1} and the electron transfer activation energy of 16.56 kJ mol^{-1}, the rate-determining step for $Fe^{III}EDTA$ reduction was diffusion step. Potentiostatic electrolysis tests revealed that direct electrochemical regeneration of $Fe^{II}EDTA$ in the wet process of NO removal was a promising method because of its high efficiency.

Keywords: Nitric oxide; Reversibility; Direct electrochemical regeneration; Activation energy

1. Introduction

The emission of nitric oxides NO_x causes the problems of acid rain and ozone destruction [1]. At present the most widespread NO_x reduction technology is the selective catalytic reduction (SCR) process, in which NO_x are removed effectively [2,3]. However, it suffers from the shortcomings of high temperature, catalysts deactivation and operation costs [4–6]. Wet process of NO_x is a promising method since it promotes the studies on simultaneous absorption of NO and SO_2. Its obstacle lies in low solubility of NO in water. Some chemical reagents such as $Fe^{II}EDTA$ [7], $NaClO_2$ [8–10], etc. were added into this system to improve NO_x absorption. Among them wet process of NO_x by means of complexes, such as $Fe^{II}EDTA$, is a highly effective method since the metal complex solution rapidly reacts with the absorbed NO to form metal–nitrosyl complexes [11]. However, the formed $Fe^{II}EDTA(NO)$ and $Fe^{III}EDTA$ lead to the invalidation of the absorption solution. As a consequence, the regeneration of absorption solution becomes a fundamental part of this method. Various reducing agents such as polyphenolic compounds [12], $Na_2S_2O_4$ [13] and Na_2SO_3 [7] have been tested. They proved to be effective but were not to be commercialized widely.

Electrochemical regeneration is a process which reduces absorption solution and converts pollutants into nontoxic compounds through electrochemical oxidation or reduction without consumption of large amount of chemicals [14]. There had been some efforts focused on the conversion of $Fe^{II}EDTA(NO)$ formed from $Fe^{II}EDTA$ and Fe^{II}(DMPS) [15], a newly synthesized compound to absorb NO. In the previous researches [16], the electrochemical oxidation process was performed after NO broke away from complexes and interacted with water. Similarly, cathodic reduction of the bound complexes had also been studied [17]. Further detailed investigations on the possibility of direct electrochemical conversion of $Fe^{II}EDTA(NO)$ were also carried out [18].

Nevertheless, it should be noted that less attention has been paid to electrochemical reduction of $Fe^{III}EDTA$ which was simultaneously produced in the course of NO absorption by $Fe^{II}EDTA$. Besides, the previous works paid more attention to elucidate the overall reactions of the complex formation rather than kinetic studies despite that kinetic study might guide us to deeply understanding the reaction mechanism. In the present work, the regeneration of $Fe^{II}EDTA$ by electrochemical approaches together with investigation on kinetic parameters of $Fe^{III}EDTA$ was analyzed by techniques of cyclic voltammetry, quasi-state polarization curve

* Corresponding author. Tel.: +86 571 8795 1771; fax: +86 571 8795 1771.
E-mail address: weirong@mail.hz.zj.cn (W.R. Zhao).

1385-8947/$ – see front matter © 2007 Elsevier B.V. All rights reserved.
doi:10.1016/j.cej.2007.09.025

Nomenclature

A	electrode area (cm^2)
B	pre-exponential factor
C	concentration ($mol\,dm^{-3}$)
D	diffusion coefficient ($cm^2\,s^{-1}$)
D_O	diffusion coefficient of oxidation state ($cm^2\,s^{-1}$)
D_R	diffusion coefficient of reduction state ($cm^2\,s^{-1}$)
E_a	apparent activation energy ($kJ\,mol^{-1}$)
E_D	diffusion activation energy ($kJ\,mol^{-1}$)
E_e	activation energy caused by electron transfer ($kJ\,mol^{-1}$)
E_P	peak potential (V)
$E_{P/2}$	half peak potential (V)
F	Faraday constant (C)
i	current (A)
i_p	peak current (A)
i_{pa}	anodic peak current (A)
i_{pc}	cathodic peak current (A)
k^0	standard rate constant ($cm\,s^{-1}$)
P	air pressure (atm)
R	ideal gas constant ($J\,mol^{-1}\,K^{-1}$)
t	time (s)
T	absolute temperature (K)
V	volume (m^3)

Greek symbols

α	transfer coefficient
η	overpotential (V)
Ψ	function associated with reversibility

and potentiostatic step method for the purpose of probing rate-determining step and further understanding the conversion of $Fe^{III}EDTA$.

2. Experimental

$Fe^{II}EDTA$ solution (0.01 M) was prepared by adding equimolar amount of $FeSO_4{\cdot}7H_2O$ and Na_2EDTA into deionized water. In order to avoid oxidation of ferrous ion, EDTA solution was deaerated 30 min under a steady nitrogen flow before the ferrous salt was fed into the volumetric flask. 0.01 M $Fe^{III}EDTA$ solution was prepared by adding $Fe_2(SO_4)_3$ into Na_2EDTA in the same manner.

$Fe^{II}EDTA(NO)$ was formed by bubbling 500 ppm NO into 0.01 M $Fe^{II}EDTA$ solution. The concentration of NO was analyzed by Saltzman method [19] and was tested with spectrophotometer 722S (Lengguang Tech., China) at the wavelength of 540 nm. The formed $Fe^{II}EDTA(NO)$ was also measured by spectrophotometer 722S at the wavelength of 420 nm [20]. The concentrations of ferrous ion and ferrite ion were determined by 1,10-phenanthroline method [21]. The concentration of NO_3^- and NO_2^- were tested by ion chromatogram (Dionex ICS-90).

Electrochemical measurements were depicted by Potentiostat/Galvanostat (EG & model 273A) in a three-electrode glass cell. Na_2SO_4 (0.5 M) was added into solution as supporting electrolyte. The reference electrode was a saturated calomel electrode (SCE) with a luggin capillary probe placed near the working electrode surface to minimize the ohmic drop through the cell. The working electrode with area 10.02 cm^2 and the counter electrode were both platinum foils. All the potential quoted in this paper were referred to the saturated calomel electrode (SCE) unless special identification.

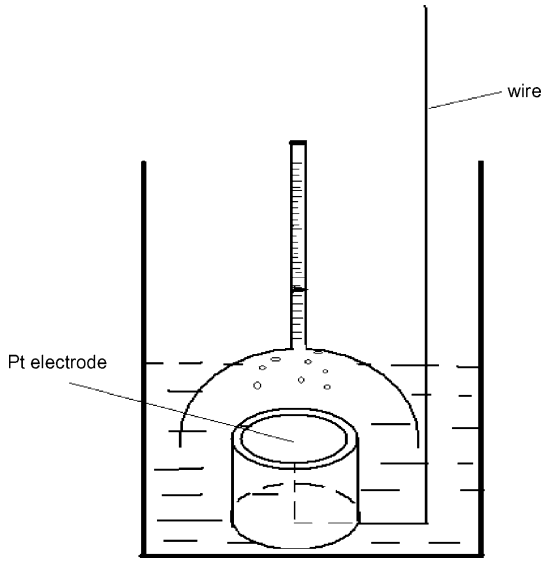

Fig. 1. The sketch map of hydrogen collection apparatus.

Hydrogen collection was performed by hydrogen collection method. The sketch map of hydrogen collection apparatus was shown in Fig. 1. The cupric wire was covered with insulated rubber. The working electrode, with its working surface exposed to solution, was encapsulated by epoxy resin. The hydrogen gas escaped from the Pt surface could be collected in a graduate glass tube. The volume of hydrogen gas could be read from the difference of solution volume in glass tube.

3. Results and discussion

3.1. Characteristics studies of electrode reactions

3.1.1. The reversibility of $Fe^{III}EDTA/Fe^{II}EDTA$ and determination of electron transfer number

Cyclic voltammetry was used to test the reversibility of $Fe^{III}EDTA/Fe^{II}EDTA$. Scan range was chosen from −0.3 to 0.6 V for the clear peak appearance. Fig. 2 illustrates the cyclic voltammograms of 0.01 M $Fe^{III}EDTA$ solution at various scan rates, in which the anodic peaks around potential 0.05 V and cathodic peaks around potential −0.06 V suggested that the process seemed reversible on account of the symmetry between the cathodic peaks and anodic peaks. A typical voltammetric curve at the scan rate of 1 $mV\,s^{-1}$ was exhibited in the inserted Fig. 2A, in which $|i_{pa}|/|i_{pc}| = 0.94$. This value was approximately 1, demonstrating that the process was a reversible one.

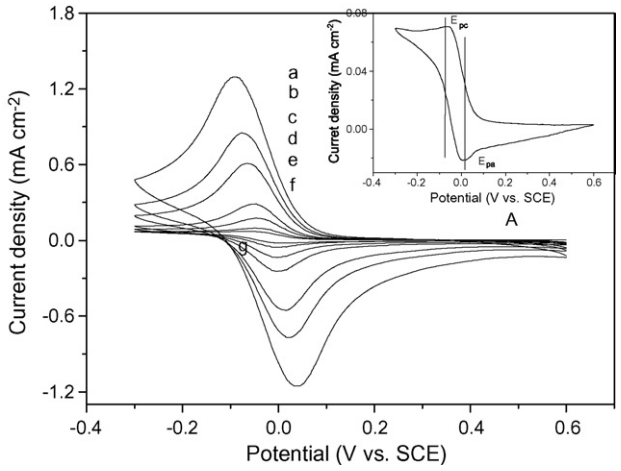

Fig. 2. Cyclic voltammograms of 0.01 M $Fe^{III}EDTA$ with Pt electrode at various scan rates: (a) 100 mV s^{-1}, (b) 50 mV s^{-1}, (c) 30 mV s^{-1}, (d) 10 mV s^{-1}, (e) 5 mV s^{-1}, (f) 2 mV s^{-1}, and (g) 1 mV s^{-1}, $C_{Na_2SO_4}$ = 0.5 M. (Inset (A)) Cyclic voltammogram of 0.01 M $Fe^{III}EDTA$ at scan rate 1 mV s^{-1}, T = 298 K.

Furthermore, the transferred electron number in a reversible electrochemistry system could also be determined by

$$|E_P - E_{P/2}| = \frac{2.2RT}{nF} \quad (1)$$

According to Fig. 2A, E_{PC} and $E_{PC/2}$ were −0.0685 and −0.0045 V. $|E_{PC} - E_{PC/2}|$ equalled 64 mV. Electron number n was calculated as 0.91. Moreover, the n values obtained at various scan rates were also deduced and the results were listed in Table 1. It could be seen that n values were close to 1 even at high scan rates. This confirmed that the conversion of $Fe^{III}EDTA/Fe^{II}EDTA$ was a reversible process with monoelectron transfer. The corresponding electron transfer equation could be expressed as follows:

$$Fe^{III}EDTA + e^- = Fe^{II}EDTA \quad (2)$$

3.1.2. Determination of standard rate constant k^0

For further determination of standard rate constant k^0 at 298 K, the diffusion coefficients of D_O and D_R were necessary. The diffusion coefficient D_O for $Fe^{II}EDTA$ could be calculated by using the Randles-Sevcik equation [22]:

$$I_p = \frac{0.4463(nF)^{3/2}ACD^{1/2}}{(RT)^{1/2}} v^{1/2} \quad (3)$$

Plots of the peak currents i_{pa} and i_{pc} versus the scan rate $v^{1/2}$ for $Fe^{III}EDTA/Fe^{II}EDTA$ at different temperatures were depicted in Fig. 3. According to Fig. 3 and Eq. (3), the diffusion coefficient D_R could be obtained as 1.68×10^{-6} cm^2 s^{-1} at 298 K. Similarly, the diffusion coefficient D_O was calculated as 2.34×10^{-6} cm^2 s^{-1}.

Table 1
The n values at various scan rates in 0.01 M $Fe^{II}EDTA$

Scan rate (mV s^{-1})	n
1	0.910
2	0.878
5	0.870
10	0.854
30	0.833
50	0.816
100	0.754

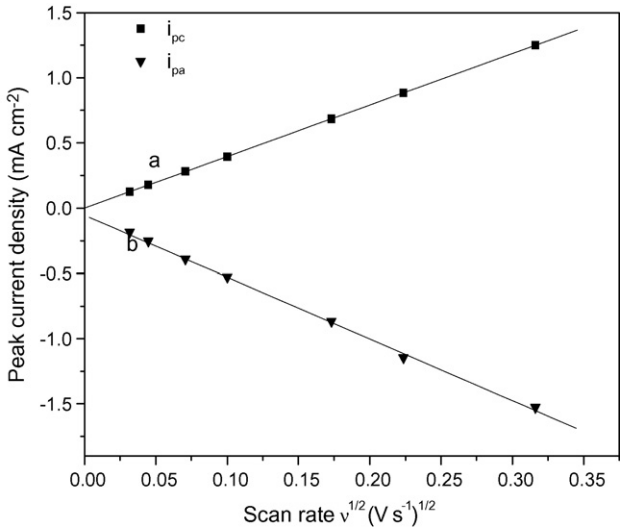

Fig. 3. Plots of i_{pa} vs. $v^{1/2}$ for 0.01 M $Fe^{II}EDTA$ and i_{pc} vs. $v^{1/2}$ for 0.01 M $Fe^{III}EDTA$, T = 298 K, $C_{Na_2SO_4}$ = 0.5 M.

To determine the standard rate constant k^0, Tafel polarization curve with a well-defined Tafel linear range was applied to evaluate transfer coefficient α. With the obtained cathodic Tafel slope 0.168, α could be subsequently calculated as 0.39 from

$$\frac{2.303RT}{(\alpha nF)} = 0.168 \quad (4)$$

Moreover, k^0 could be expressed as Eq. (5) [23]:

$$\psi = \frac{(D_O/D_R)^{\alpha/2}k^0}{((\pi D_O nF)/RTv)^{1/2}} \quad (5)$$

When α was in the range of $0.3 < \alpha < 0.7$, Ψ was only related to ΔE_P, which could be known from cyclic voltammogram. Thus Ψ could be deduced at the corresponding scan rate [24]. From the values of D_O, D_R and Ψ, standard rate constant k^0 at 298 K could be calculated as 0.0263 cm s^{-1}. The value of k^0 was more than 10^{-2} cm s^{-1}, indicating that the reduction process of $Fe^{III}EDTA$ was a fast reversible one.

3.2. Studies on rate-determining step

A complete electrochemical reaction process at least includes the diffusion step and the electron transfer step. The diffusion step is a process with electroactive species transferred from electrolyte solution to electrode interface, while the electron transfer step is an electrochemical reaction process on electrode surface. In Fig. 2 the cathodic peaks and anodic peaks rose steeply and decayed slowly, indicating that the electrode reaction was mainly controlled by diffusion step. Diffusion activation energy, apparent activation energy and activation energy caused by electron transfer were investigated in order to confirm the rate-determining step.

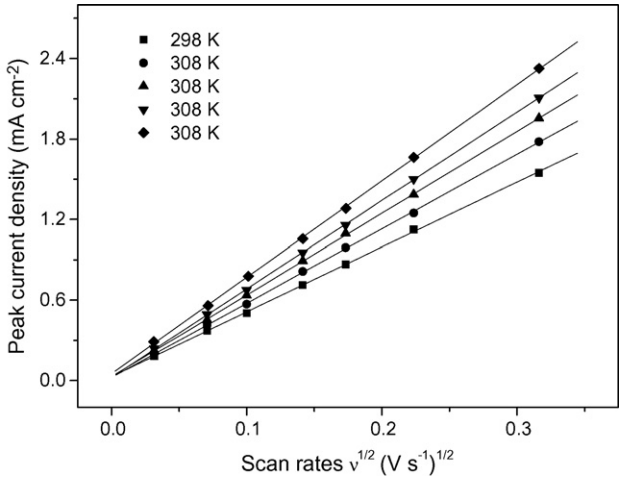

Fig. 4. Plots of i_{pc} vs. $v^{1/2}$ for 0.01 M $Fe^{III}EDTA$ at various temperatures and scan rates, $C_{Na_2SO_4} = 0.5$ M.

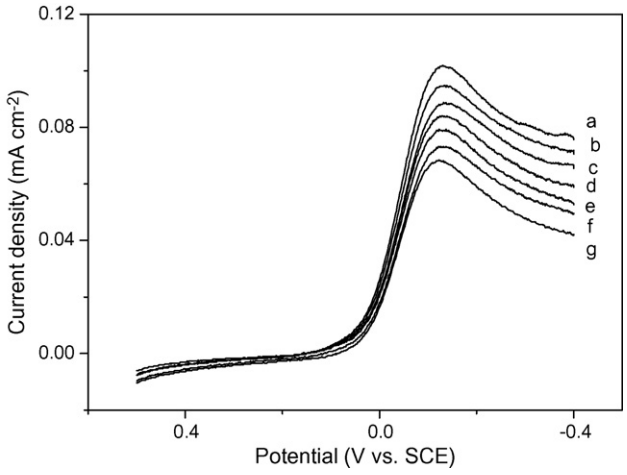

Fig. 6. Quasi-steady-state polarization curves of $Fe^{III}EDTA$ at different temperatures: (a) 328 K, (b) 323 K, (c) 318 K, (d) 313 K, (e) 308 K, (f) 303 K, and (g) 298 K. Scan rate = 1 mV s^{-1}, $C_{Na_2SO_4} = 0.5$ M.

3.2.1. Studies on diffusion activation energy

Diffusion activation energy E_D was expressed as

$$\ln D_R = \ln B + \frac{-E_D}{RT} \tag{6}$$

According to Eq. (3), the scan rate dependence of cathodic peak current i_{pc} at various temperatures was tested and the results were shown in Fig. 4. Then D_R changed with temperature could be deduced. The relationship between $\ln D_R$ and $1/T$ was depicted in Fig. 5. Diffusion activation energy E_D that $Fe^{III}EDTA$ diffused to Pt electrode was 24.93 kJ mol^{-1} according to the slope of Fig. 5 and Eq. (6).

3.2.2. Determination of apparent activation energy

Quasi-steady-state polarization curve, a steady-state method was used to calculate the apparent activation energy of $Fe^{III}EDTA/Fe^{II}EDTA$ conversion. It was known that the current was related to the temperature by Eq. (7), where E was activation energy:

$$\left[\frac{\partial \ln i}{\partial T}\right]_\eta = \frac{E}{RT^2} \tag{7}$$

From Eq. (7), the apparent activation energy E_a was integrated as follows:

$$E_a = \frac{2.303R(\lg i_2 - \lg i_1)}{(1/T_1) - (1/T_2)} \tag{8}$$

The currents of quasi-steady-state polarization curve at various temperatures were given in Fig. 6. The limit currents appeared approximately at −0.14 V. The relationship between $\lg i$ and $1/T$ was shown in Fig. 7 at the same overpotential ($E = -0.14$ V), in which it was found that $\lg i$ was a linear function of $1/T$. From the slope of such plots the apparent activation energy was calculated as 25.74 kJ mol^{-1}. The fact that E_D was almost equal to E_a indicated that the whole reaction was mainly dominated by diffusion step.

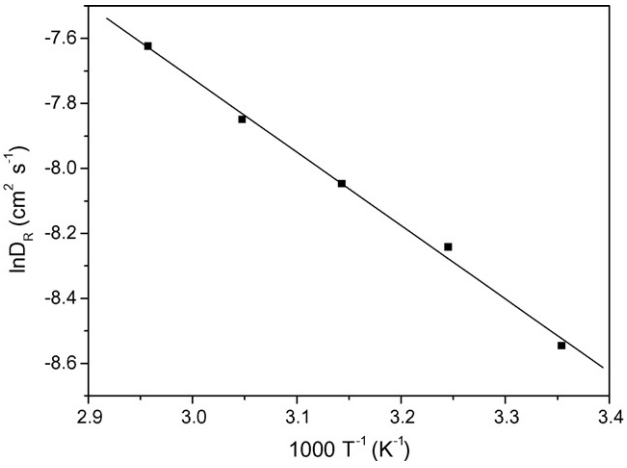

Fig. 5. Plots of $\ln D_R$ vs. $1000T^{-1}$ for 0.01 M $Fe^{III}EDTA$ solution.

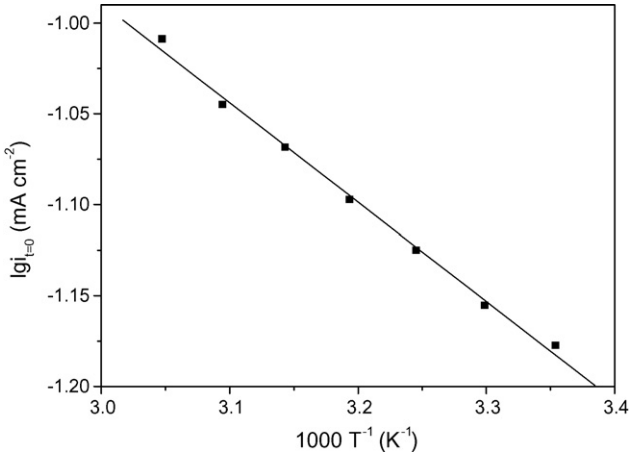

Fig. 7. Plots of $\lg i_{t=0}$ vs. $1000T^{-1}$ at various temperatures for 0.01 M $Fe^{III}EDTA$ solution, scan rate = 1 mV s^{-1}.

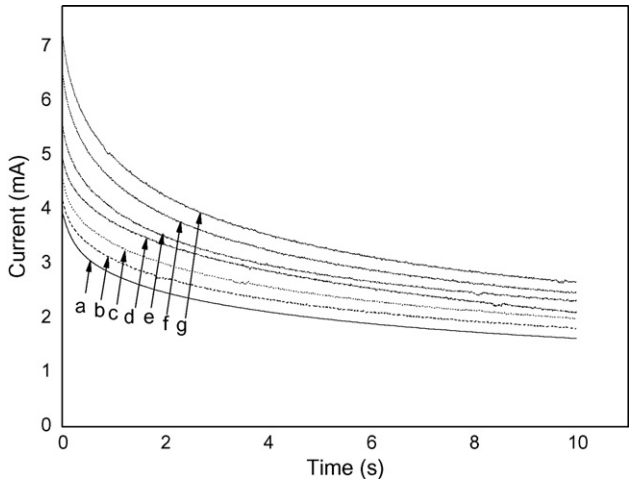

Fig. 8. The potentiostatic step plots 0.01 M $Fe^{III}EDTA$ solution at various temperatures: (a) 298 K, (b) 303 K, (c) 308 K, (d) 313 K, (e) 318 K, (f) 323 K, and (g) 328 K, $C_{Na_2SO_4} = 0.5$ M.

3.2.3. Determination of activation energy caused by electron transfer step

In avoid of the concentration polarization the transient method of potentiostatic step was applied to study the activation energy caused by electron transfer. The limit currents appeared at −0.14 V. So this potential was selected to perform potentiostatic step curves at different temperatures, as described in Fig. 8. Since concentration polarization could be ignored in a very short time (less than 0.1 s), the relationship between i and $t^{1/2}$ was linear. As a consequence, the various $i_{t=0}$ values could be deduced from the intercepts of fit lines at corresponding temperatures. Temperature dependence of lg $i_{t=0}$ was illustrated in Fig. 9. It could be seen that the plots of lg $i_{t=0}$ versus $1/T$ was linear. Activation energy E_e caused by electron transfer without influence of concentration diffusion was calculated as 16.56 kJ mol^{-1} according to Eq. (7). The value of activation energy E_e was 9.18 kJ mol^{-1} less than that of apparent activation energy. From above discussion we drew the conclusion again that the reduction of $Fe^{III}EDTA$ on Pt electrode was dominated by diffusion step.

3.3. Studies on the direct electrochemical reduction

On the premise that the productions of $Fe^{III}EDTA$ and $Fe^{II}EDTA(NO)$ accompanied NO absorption, the practical reduction results were examined by bubbling 500 ppm NO into 0.01 M $Fe^{II}EDTA$ solution. Equilibrium was reached when inlet NO concentration was equal to outlet NO concentration. Cyclic voltammetric behaviors of $Fe^{II}EDTA$ and $Fe^{II}EDTA(NO)$ solution and the electrochemical reduction products had been analyzed before [25]. Since high negative potential increased the reduction rate of $Fe^{III}EDTA$, and caused some side reactions, e.g. hydrogen evolution, the three typical potentials −0.3, −0.7 and −1.1 V were selected as the potentiostatic potentials to analyze the reduction in more details. The total electron quantities could be calculated by integrating potentiostatic i–t curves at various potentials. Hydrogen evolution quantity was obtained by hydrogen collection apparatus. Transferred electron quantities of $Fe^{III}EDTA$, $Fe^{II}EDTA(NO)$ and NO_2^- et al. could be calculated through measured concentration changes before and after reduction and electron transfer number n according to Eqs. (2), (8) and (9):

$$Fe^{II}EDTA(NO) + e + H^+ = Fe^{II}EDTA + N_2O + H_2O \quad (8)$$

$$6H^+ + 2NO_2^- + 4e = N_2O + H_2O \quad (9)$$

Fig. 10 shows potentiostatic reduction curves at −0.3, −0.7 and −1.1 V on Pt electrode, from which reduction electron quantities could be obtained. At −0.3, −0.7 and −1.1 V, 93.55, 58.87 and 17.29% of total electron quantities were transferred to reduce $Fe^{III}EDTA$, meanwhile, 1.13, 28.94 and 10.45% of total electron quantities were transferred to reduce $Fe^{II}EDTA(NO)$, respectively. Side reactions mainly comprised hydrogen reductions and NO_2^- reduction. Total electron quantities (3.72 and 64.38%) were consumed to produce hydrogen at −0.7 and −1.1 V separately, and 3.54, 5.50 and 4.36% of total electron

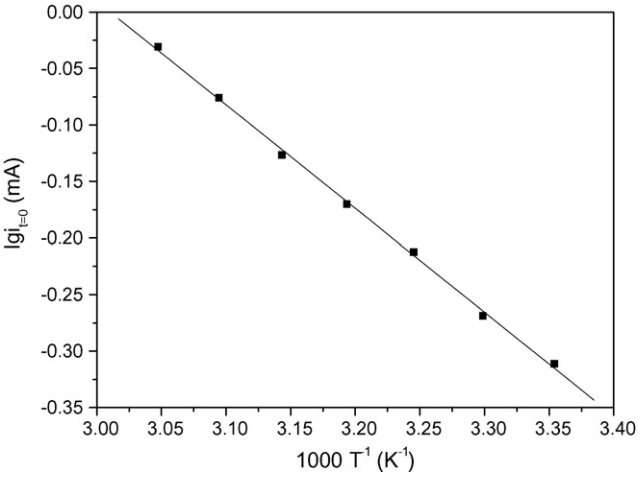

Fig. 9. Plots of lg $i_{t=0}$ vs. $1000T^{-1}$ for 0.01 M $Fe^{III}EDTA$ solution at various temperatures.

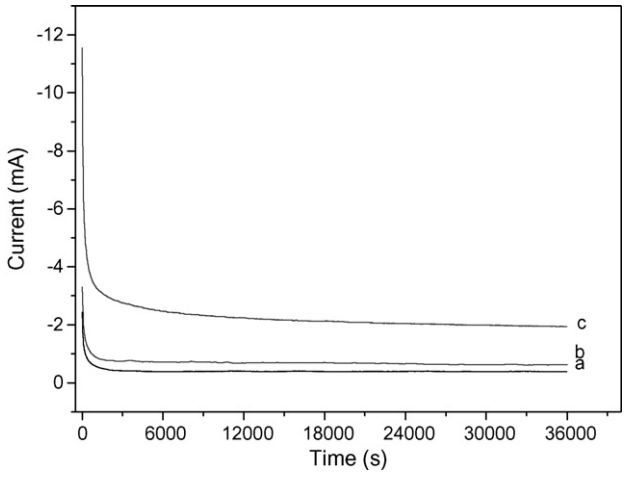

Fig. 10. Potentiostatic reduction curves of NO-equilibrated solution in 0.01 M $Fe^{II}EDTA$ on Pt electrode: (a) −0.3 V, (b) −0.7 V, and (c) −1.1 V, $T = 298$ K, $C_{Na_2SO_4} = 0.5$ M.

quantities were used to reduce NO_2^- at −0.3, −0.7 and −1.1 V as well. Some other side reactions might include oxygen reduction.

4. Conclusions

The direct electrochemical reduction of $Fe^{III}EDTA$ produced in NO absorption by $Fe^{II}EDTA$ solution demonstrated that the conversion of $Fe^{III}EDTA$ into $Fe^{II}EDTA$ was a fast reversible process with monoelectron transferred. Standard rate constant k^0 at 298 K was 0.0263 cm s^{-1}. Kinetic parameters of diffusion activation energy 24.93 kJ mol^{-1}, apparent activation energy 25.74 kJ mol^{-1} and activation energy 16.56 kJ mol^{-1} caused by electron transfer process confirmed that the reduction of $Fe^{III}EDTA$ was mainly controlled by diffusion process.

Direct electrochemical regeneration $Fe^{III}EDTA$ was investigated over a wide range of potential. It was found that electrons were mainly transferred to reduce $Fe^{III}EDTA$ at −0.3 V. At −0.7 and −1.1 V $Fe^{II}EDTA(NO)$ was found decomposed at the same time. Generally speaking, direct electrochemical reduction provided a promising method to regenerating $Fe^{II}EDTA$ in the wet process of NO absorption.

Acknowledgments

This work was supported by New Century Excellent Human Resource Training Project of Ministry of Education (NCET04-0549) and Zhejiang Provincial Science and Technology Foundation (2004C23028). The author also gratefully acknowledges Dr Jun-bo Wang for his helpful discussion.

References

[1] Y.S. Mok, I.S. Nam, Modeling of pulsed corona discharge process for the removal of nitric oxide and sulfur dioxide, Chem. Eng. J. 85 (2002) 87–97.
[2] J.D. Wang, C.Q. Wu, J.M. Chen, H.J. Zhang, Denitrification removal of nitric oxide in a rotating drum biofilter, Chem. Eng. J. 121 (2006) 45–49.
[3] I.Y. Lee, D.W. Kim, J.B. Lee, K.O. Yoo, A practical scale evaluation of sulfated V_2O_5/TiO_2 catalyst from metatitanic acid for selective catalytic reduction of NO by NH_3, Chem. Eng. J. 90 (2002) 267–272.
[4] X.L. Long, W.D. Xiao, W.K. Yuan, Simultaneous absorption of NO and SO_2 into hexamminecobalt(II)/iodide solution, Chemosphere 59 (2005) 811–817.
[5] C.H. Tsai, H.H. Yang, C.J.G. Jou, H.M. Lee, Reducing nitric oxide into nitrogen via a radio-frequency discharge, J. Hazard. Mater. 143 (2007) 409–414.
[6] N.A.S. Amin, C.M. Chong, SCR of NO with C_3H_6 in the presence of excess O_2 over $Cu/Ag/CeO_2–ZrO_2$ catalyst, Chem. Eng. J. 113 (2005) 13–25.
[7] E. Sada, H. Kumazawa, Y. Takada, Chemical reactions accompanying absorption of NO into aqueous mixed solutions of Fe(II)-EDTA and sodium sulfite, Ind. Eng. Chem. Fund. 23 (1984) 60–64.
[8] H. Chu, T.W. Chien, B.W. Twu, The absorption kinetics of NO in $NaClO_2/NaOH$ solutions, J. Hazard. Mater. 84 (2001) 241–252.
[9] B.R. Deshwal, H.K. Lee, Kinetics and mechanism of chloride based chlorine dioxide generation process from acidic sodium chlorate, J. Hazard. Mater. 108 (2004) 173–182.
[10] S. Lee, K. Park, J.W. Park, B.H. Kim, Characteristics of reducing NO using urea and alkaline additives, Combust. Flame 141 (2005) 200–203.
[11] T. Schneppensieper, S. Finkler, A. Czap, R. van Eldik, M. Heus, P. Nieuwenhuizen, C. Wreesmann, W. Abma, Tuning the reversible binding of NO to iron(II) aminocarboxylate and related complexes in aqueous solution, Eur. J. Inorg. Chem. (2001) 491–501.
[12] M.H. Mendelsohn, J.B.L. Harkness, Enhanced flue-gas denitrification using ferrous-EDTA and a polyphenolic compound in an aqueous scrubber system, Energy Fuels 5 (1991) 244–248.
[13] T.T. Suchecki, B. Mathews, H. Kumazawa, Kinetic study of ambient-temperature reduction of FeβEDTA by $Na_2S_2O_4$, Ind. Eng. Chem. Res. 44 (2005) 4249–4253.
[14] K.H. Kleifges, E. Juzeliùnas, K. Juttner, Electrochemical study of direct and indirect NO reduction with complexing agents and redox mediator, Electrochim. Acta 42 (1997) 2947–2953.
[15] E.K. Pham, S.G. Chang, Removal of NO from flue gases by absorption to an iron(II) thiochelate complex and subsequent reduction to ammonia, Nature 369 (1994) 139–141.
[16] K. Ogura, T. Ozeki, Mechanism of FeNO-EDTA complex formation and its oxidization, Electrochim. Acta 26 (1981) 877–882.
[17] K. Kusakabe, H. Nishida, S. Morooka, Simultaneous electrochemical removal of copper and chemical oxygen demand using a packed-bed electrode cell, J. Appl. Electrochem. 16 (1986) 121–125.
[18] E. Juzeliùnas, K. Juttner, Electrochemical study of NO conversion from Fe(II)-EDTA-NO complex on Pt electrodes, J. Electrochem. Soc. 145 (1998) 53–58.
[19] B.E. Saltzman, Colorimetric microdetermination of nitrogen dioxide in the atmosphere, Anal. Chem. 26 (1951) 1949–1955.
[20] D. Littlejohn, S.G. Chang, Kinetic study of ferrous nitrosyl complexes, J. Phys. Chem. 86 (1982) 537–540.
[21] A.E. Harvey Jr., F.A. Smart, E.S. Aims, Simultaneous spectrophotometric determination of iron(II) and total iron with 1,10-phenenthroline, Anal. Chem. 27 (1955) 26–29.
[22] R.S. Nicholson, Theory and application of cyclic voltammetry for measurement of electrode reaction kinetics, Anal Chem. 37 (1965) 1351–1355.
[23] M.V. Mirkin, A.J. Bard, Simple analysis of quasi-reversible steady-state voltammograms, Anal. Chem. 64 (1992) 2293–2302.
[24] R.S. Nicholson, I. Shain, Theory of stationary electrode polarography: single scan and cyclic methods applied to reversible, irreversible, and kinetic systems, Anal. Chem. 36 (1964) 706–723.
[25] L. Wang, W.R. Zhao, Z.B. Wu, Simultaneous absorption of NO and SO_2 by $Fe^{II}EDTA$ combined with Na_2SO_3 solution, Chem. Eng. J. 132 (2007) 227–232.